Structural Aspects of Lyotropic Solvation-Induced Transitions in Phosphatidylcholine and Phosphatidylethanolamine Assemblies Revealed by Infrared Spectroscopy

H. Binder*,† and W. Pohle‡

University of Leipzig, Institute of Medical Physics and Biophysics, Liebigstrasse 27, D-04103 Leipzig, Germany, and Friedrich-Schiller-University Jena, Institute of Molecular Biology, Winzerlaer Strasse 10, D-07745 Jena, Germany

Received: March 28, 2000; In Final Form: August 24, 2000

The hydration of two peculiar unsaturated lipids with phosphatidylethanolamine (PE) and phosphatidylcholine (PC) headgroups, namely dioctadecadienoyl PC (DODPC) and dioleoyl PE (DOPE), has been studied at room temperature by infrared (IR) spectroscopy including the linear dichroism. Oriented films of these lipids subjected to an atmosphere with definite values of relative humidity were investigated. The choice of DODPC and DOPE was motivated by their common property of undergoing a lyotropic phase transition, which, in each case, nearly exclusively affects the polar part of the lipid aggregates and is, thus, termed "solvation-induced" transition. The temperature−RH phase diagrams of both lipids were determined. The headgroups of both lipids form quasi-crystalline structures at small RH. The long axes of the PE and PC moieties orient essentially parallel with respect to the polar interface of the lipid aggregates. Model-based analyses of IR linear-dichroism data are consistent with the idea that about 8−12 DOPE molecules with disordered chains assemble within one cross-section layer of a ribbonlike phase, P_α. Dry DODPC forms a subgel phase (SG_I) with all-trans acyl chains. At a critical water activity near 0.6, the molecular disorder in the polar region of the lipid aggregates increases distinctly. This "headgroup melting" reflects the solvation-induced transitions leading to the SG_{II} and H_{II} phases in DODPC and DOPE, respectively. Hydrogen-bonding specifics due to the polar parts of both lipids were probed by means of H → D exchange. Particularly stable H bonds are indicated to exist in dried DOPE.

Introduction

Phospholipids with choline (PC) and ethanolamine (PE) headgroups constitute major portions of plasma membranes. With rat-liver cells as a typical example, as much as 39% PC and 23% PE contribute to their lipid fraction (see ref 1 and references therein). Presumably due to a regulatory principle, PCs are mainly located in the outer leaflet of the lipid bilayer whereas PE lipids are mainly found in the inner monolayer. PC headgroups are known to be well hydrated and their hydration shell prevents opposing membranes and macromolecules, such as proteins, from approaching.

The nature of the short-range forces acting near the polar region of phospholipid bilayers has attracted considerable interest for a long time since it is directly related to functional concepts of cellular membranes, such as their potency to fuse.[2−5] The mechanism by which the interfacial region affects the state of lipid aggregates is yet unclear in several respects. The chemically heterogeneous and highly anisotropic interfacial layers of membranes existing between bulk−water phases and hydrocarbon cores seem to be more alike to a continuum of "polarities" gradually transforming to "hydrophobicities" that bridges the gap between the polar and apolar regions than to a simple "oil−water" boundary.[6] Under physiological conditions, the headgroups are well solvated and the polar region is therefore highly flexible. In lipid aggregates, the amplitudes of fluctuations at an interface depend crucially on the character and the strength of relevant intermolecular interactions as mediated by the solvent. Moreover, it has been recognized that repulsive forces between membranes arise between disordered surfaces where the entropy is essential.[7] The factors that generate short-range forces between amphiphilic interfaces are based on direct surface−water, surface−surface and water−water interactions.[2] Altogether, these interactions give rise to a sort of "chemical" hydration that involves all surface−water hydrogen bonds and so-called salt bridges, meaning charge pairs that form when oppositely charged groups come in close contact.[8]

Referring to the inner leaflet of biological membranes, they are rather suitable to associate a number of proteins or peptides. Direct interactions between the lipids and such additives play an essential role in stabilizing these contacts since, besides the hydrophobic effect and electrostatic interactions, hydrogen bonds represent an important option to determine the specifics of the particular structure formed. The affinity of a macromolecule to the lipid matrix is governed after all by the thermodynamic gain upon replacing direct lipid−lipid and lipid−water interactions by cross interactions between the lipid and the additive. Partitioning of proteins and peptides into the highly flexible region given by the polar domain of lipid assemblies will follow the physicochemical gradient and disposition that yields the largest reduction in free energy. The location adopted finally in the membrane will depend on the balance between hydrophobic as well as polar and electrostatic effects and hydrogen bonds. Hydration water and various aspects of the hydration process obviously play a central role for the essential properties of membrane-bound proteins.[9]

* To whom correspondence should be addressed. E-mail: binder@rz.uni-leipzig.de. Fax: +49-341-9715709.
† University of Leipzig.
‡ Friedrich-Schiller-University Jena.

10.1021/jp0011793 CCC: $19.00
Published on Web 11/28/2000

Physical-chemical studies of several lipids performed at room temperature as a function of hydration, which has been adjusted and varied in an atmosphere of well-defined relative humidity, RH, have revealed the existence of lyotropic phase transitions quite different in nature.[10−15] Some of the studied lipids, such as DODPC, POPC or OPPC, undergo, upon water binding, lyotropic chain-melting (main) transitions that are mainly characterized by changes in the hydrophobic region of the lipid aggregates. In two particular cases, however, more exotic lyotropic phase transitions have been observed. This concerns two unsaturated phospholipids with either a choline or an ethanolamine headgroup, namely dioctadecadienoyl PC (DODPC) and dioleoylphosphatidyl PE (DOPE). Progressive hydration induces phase transitions in the aggregates of these lipids that comprise two lamellar subgel phases (SG_I and SG_{II}) and two nonlamellar phases (P_α and H_{II}), respectively. In the following, these lyotropic phase transitions will be denominated headgroup-solvation or, for short, solvation-induced transitions since they nearly exclusively affect the polar region of the lipids.[11,14,16,17] This feature attracts special interest because it allows us to study details of the molecular interactions occurring upon PE and PC hydration without a noticeable interference from the hydrophobic core. Moreover, it gives an opportunity to compare the solvation characteristics of both headgroup types, which is of fundamental interest because of their potency to form markedly different hydrogen-bonding patterns.[18]

The main purpose of the present study is to obtain a definite picture of the polar region of the lipids involving structural, thermodynamic (i.e., enthalpic and entropic) and kinetic aspects. For the sake of clarity this work is organized in two parts. In the first part, we report data obtained by Fourier transform infrared (FTIR) spectroscopy and, in particular, IR linear dichroism. This method yields detailed information about the aggregate structure and architecture on a molecular level as has been proven for DODPC in previous studies devoted to its lyotropic properties.[11,16,17] These data will be supplemented in the present study. However, the focus will be directed more onto DOPE, which was not so comprehensively characterized up to now. DOPE is known for its propensity to form nonlamellar structures; this holds also for the states adopted before and after the solvation-induced transition discussed here.[14,19] Hence, we examine the question how to analyze IR linear dichroism data of nonlamellar structures. The thermodynamics and kinetics of headgroup solvation will be dealt with in the accompanying second paper.[20]

Experimental Section

Materials. For the preparation of lipid films we used stock solutions of the lipids DOPE (1,2-dioleoyl-*sn*-glycerophosphatidylethanolamine; from Sigma Co., Munich, Germany) and DODPC (1,2-bis(2-*trans*-4-*trans*-octadecadienoyl)-*sn*-glycerophosphatidylcholine; Nippon Oil and Fats Co., Japan) in methanol (∼5−20 mM).

Infrared Measurements. Films of the lipids were prepared by pipetting 100−200 μL of the stock solution on the surface of a ZnSe attenuated total reflection (ATR) crystal (angle of incidence: 45°, six active reflections) and evaporating the solvent under a stream of nitrogen. The amount of material used for preparation corresponds to an average thickness of the films of >3 μm, or equivalently, to a stack of $>10^3$ bilayers in lamellar phases. Hence, the films represent bulk samples despite the macroscopic orientation of the lipid aggregates on the surface of the ATR crystal (vide infra). The ATR crystal was mounted into a BioRad FTS-60a Fourier transform infrared spectrometer (Digilab, MA) using a commercial horizontal benchmark unit (Graseby Specac, Kent, U.K.) that had been modified to realize a definite relative humidity (RH) and temperature (T) at the crystal surface coated with the sample.[11] Polarized absorption spectra (128 accumulations each) were recorded with IR light polarized parallel, $A_\parallel(\nu)$, and perpendicular, $A_\perp(\nu)$, with respect to the plane of incidence. IR order parameters of absorption bands, $S_{IR} = (R - 2)/(R + 2.55)$, were calculated from the dichroic ratio of the integral, baseline-corrected polarized absorbances, $R = A_\parallel/A_\perp$ (see ref 21 for details of the method). Band positions were analyzed in terms of their center of gravity obtained from the weighted sum spectrum $A(\nu) = A_\parallel(\nu) + 2.55A_\perp(\nu)$.[21]

Results

FTIR Spectral Characteristics of DOPE as a Function of Hydration. Recent IR investigations showed that DOPE undergoes a lyotropic phase transition in the intermediate RH range.[14] The "high-humidity" phase is of inverse hexagonal morphology (H_{II}) according to the phase diagram of DOPE.[19,22] The "low-humidity" state was ascribed to a fluid ribbon phase, P_α (or P_{II}), which is constructed of strains of headgroup-centered lipid assemblies.[14,23] The phase transition is nearly exclusively characterized by structural reorientations within the polar part of the molecules because drastic alterations occurred only for the absorption bands due to the PE headgroup. In contrast, the methylene stretching vibration bands are nearly not affected at this transition. The symmetric and antisymmetric CH_2 stretches of DOPE are centered at 2853.5 and 2922.5 cm^{-1} before and after the phase transition, respectively. These wavenumbers are characteristic of lipids with fluid acyl chains.[24] Here we present a more detailed analysis of the IR characteristics of DOPE before and after the $P_\alpha-H_{II}$ transition to explore the structural origin of this event. IR absorption bands of PE lipids with saturated and unsaturated acyl chains were assigned previously.[12,25−27]

Figure 1 shows the absorption bands of selected vibrations of the ammonium and phosphate groups of DOPE at RH values well below and above the $P_\alpha-H_{II}$ transition (see also Table 1). The bands due to symmetric NH_3 bending, $\delta_s(NH_3)$, its combination with the CCN bending, $\{\delta(CCN) + \delta_s(NH_3)\}$ and the symmetric CCN stretching band, $\nu_s(CCN)$, protrude in the P_α phase as relatively sharp peaks. Narrow absorption bands of the ammonium groups of disaturated PEs were suggested to reflect long-lived H bonds of the N^+H_3 group with the nonesterified oxygens of the PO_2^- group, which "lock" the amine protons.[27] The split $\nu_{as}(CCN)$ band was previously assigned to $CC(NH_2)$ and $CC(NH_3^+)$ stretches at 1013 and 1002 cm^{-1}, respectively.[28,29] Thus, a proton-transfer equilibrium with the proton-limiting structures $(H_2)N^+H\cdots OP^-O$ and $(H_2)N\cdots HOPO$ possibly exists. This interpretation is in correspondence with the split antisymmetric PO_2^--stretching band in the P_α state, which can be tentatively assigned to different modes of hydrogen bonding. The appearance of the high-frequency $\nu_{as}(PO_2^-)$ shoulder at 1245 cm^{-1} is accompanied by an intense low-frequency band component due to the antisymmetric $P-(OC)_2$ ester-bond stretching mode, $\nu_{as}(P-(OC)_2)$, at 808 cm^{-1}. Taking into account that the $\nu_{as}(PO_2^-)$ and the $\nu_{as}(P-(OC)_2)$ modes shift in opposite directions with increasing H-bond formation to the water[11,14] (see below), it appears reasonable to assign the left-hand shoulder of $\nu_{as}(PO_2^-)$ and the right-hand component of $\nu_{as}(P-(OC)_2)$ to weakly H-bonded or even free phosphates. The more intense main band of $\nu_{as}(PO_2^-)$ at 1227 cm^{-1} and the left-hand component of $\nu_{as}(P-(OC))$ at 822 cm^{-1} originate probably from phosphate groups that interact via H bonds with the ammonium groups.

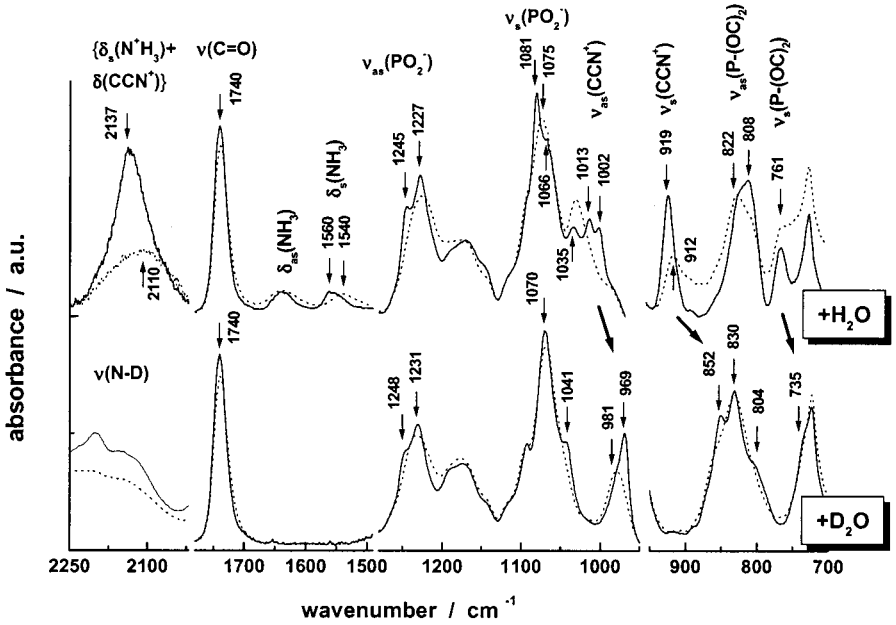

Figure 1. IR absorbance spectra of DOPE in the region of selected vibrations of ammonium, phosphate and carbonyl groups. The assignments for absorption bands are given in the figure, see also Table 1. Spectra were recorded at 25 °C and RH = 50% (solid line) and RH = 65% (dotted) in a H_2O (above) or D_2O:H_2O (9:1, below) atmosphere. These conditions correspond to DOPE before (RH = 50%) and after (RH = 65%) the P_α/H_{II} transition. The numbers give characteristic band positions in units of cm^{-1}, bold arrows indicate shifts of absorption bands owing to the H → D exchange of the ammonium groups. The symbols are defined as follows: ν, stretching vibration; δ, bending vibration; subscripts s and as, symmetric and antisymmetric modes (see text and Table 1).

TABLE 1: Assignments of Selected Vibrations of the Phosphate, Ammonium, and Carbonyl-Ester Groups of DOPE (RH = 5%, P_α Phase) and DODPC (RH = 20%, SG_I Phase), Their Wavenumbers at Maximum Absorption, and IR Order Parameters in a H_2O and D_2O:H_2O (only DOPE) Atmosphere

		DOPE				DODPC	
		H_2O		D_2O:H_2O (9:1)		SG_I	
peak	assignment [a]	position[b]/cm^{-1}	S_{IR}[c]	position[b]/cm^{-1}	S_{IR}[c]	position[d]/cm^{-1}	S_{IR}[c,d]
	phosphate						
(1)	$\nu_{as}(PO_2^-)_{1245}$	1245	0.3	1248	>0.05		
(2)	$\nu_{as}(PO_2^-)$	1227	−0.05	1231	−0.05	1255−1249	−0.25
(3)	$\nu_s(PO_2^-)$	1081	−0.2	1070	−0.1	1092	<0
(4)		1068	0.15	x			
(5)	ν(P−O(C^C))	1035	−0.25	1041		1054−1049	<−0.25
(6)	ν_{as}(P−$(OC)_2$)	822	−0.1	830	−0.15	806	−0.15
(7)	$\nu_{as}(P-(OC)_2)_{808}$	808	−0.1	803		800	
(8)	ν_s(P−$(OC)_2$)	763	−0.4	735		765	−0.1
	ammonium						
(9)	$\nu_{as}(CCN)_{1013}$	1013	−0.1	x			
(10)	ν_{as}(CCN)	1003	−0.35	969	−0.2	970[e]	−0.3...−0.4
(11)	ν_s(CCN)	920	−0.25	852		927[e]	−0.2...−0.4
	carbonyl						
(12)	ν(C═O)	1740	−0.05	1740	−0.05	1715/1700	−0.05

[a] According to refs 12 and 51. Key: ν, stretching vibration; s, symmetric; as, antisymmetric. $-C^G-O-PO_2^-$ $-O-C^C-$: C^G and C^C, carbons of the glycerol and cholin moieties, respectively. [b] Resolution: ±1 cm^{-1}. [c] Calculated after baseline correction; see ref 21. Error: ±0.05. [d] Taken from refs 11, 16, and 17. [e] $\nu_{as}(N(CH_3)_3)$ and $\nu_s(N(CH_3)_3)$ modes of the choline group; see ref 16 for details.

The absorption bands of the phosphate and ammonium groups widen considerably at the phase transition between the P_α and H_{II} phases. This phenomenon can be explained by a larger distribution of energetic states owing to different conformations and/or interactions of the respective moieties. Moreover, the shift of the phosphate bands and the disappearance of the left-hand shoulder of the $\nu_{as}(PO_2^-)$ mode give rise to the hypothesis that the degree of H bonding to the phosphate group, i.e., the fraction of phosphates with a tendency to be "saturated" by H bonds, increases at the transition. This interpretation is confirmed by the shift of the ammonium bands and the disappearance of the splitting of the antisymmetric CCN stretching band, ν_{as}-(CCN), at the phase transition (cf. Figure 1). The shift of the $\delta_s(NH_3^+)$ band from 1560 to 1540 cm^{-1} shows that the $NH_3^+\cdots PO_2^-$ interactions are loosened and/or replaced by interactions with the water owing to hydration of the ammonium and phosphate groups (see next section).[28] Obviously, at the $P_\alpha-H_{II}$ phase transition of DOPE the ordering of the PE headgroups decreases owing to their hydration.

In general, the shift and intensity changes of IR bands of the phosphate and ammonium groups reveal a complex picture that cannot be explained merely in terms of a strengthening or weakening of hydrogen bonds but includes probably conformational changes as well. Unfortunately, no direct information is available from IR spectra about the conformations of the O−P−O−C−C−N fragments.

Spectral Characteristics of DOPE after H → D Exchange. Specific information can be also obtained from the analysis of

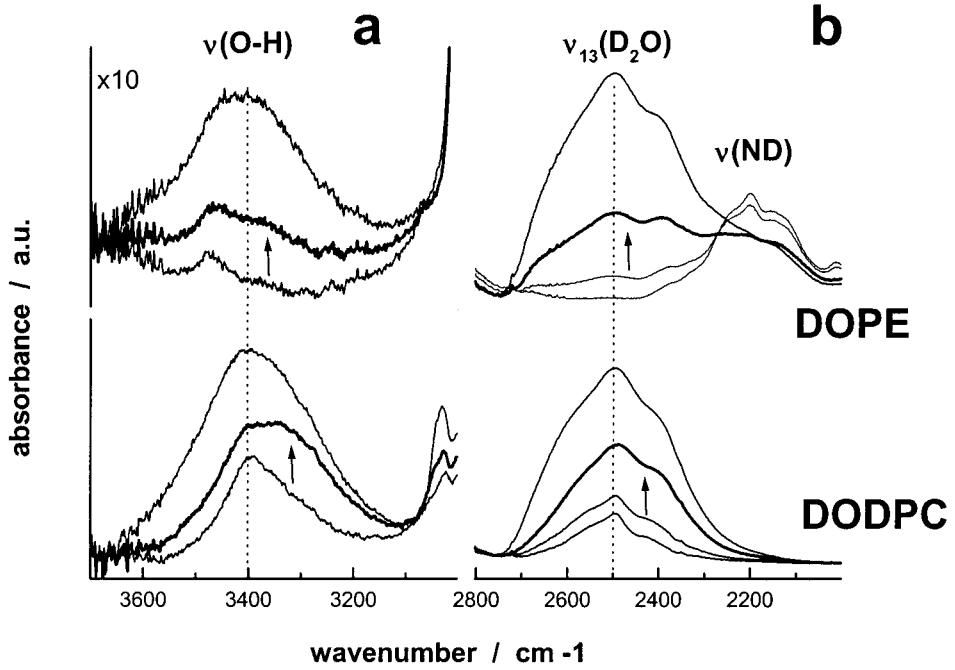

Figure 2. IR spectra of DOPE and DODPC, which were hydrated at 25 °C in an atmosphere of D_2O/H_2O vapor (9:1 mol/mol) according to RH = 20%, 50% (only right part), 65% and 89% (the intensities of the ν(OH) and $\nu_{13}(D_2O)$ bands increase with RH). Parts a and b show the spectral range of the isotopically isolated O−H stretching bands and the right part the range of the D_2O and ND_3 (ν(ND), only DOPE) stretching modes, respectively. The arrows indicate the spectral changes at the $P_\alpha-H_{II}$ (DOPE) and SG_I-SG_{II} (DODPC) phase transitions.

the O−H and N−H stretching vibration, $\nu_{13}(H_2O)$ and ν(NH), respectively, because these modes are sensitive to hydrogen bonding.[30] Unfortunately, the ν(NH) band is hidden behind the strong CH_2 stretching bands in the spectral range of 3000−2800 cm^{-1}. Hydration of the lipid with a 9:1 D_2O/H_2O mixture (mol/mol) causes the isotopic H → D exchange of the ammonium groups within several hours. The O−D and N−D stretches, $\nu_{13}(D_2O)$ and ν(ND), respectively, shift to wavenumbers in the range 2800−2000 cm^{-1}, which is nearly free of overlapping bands. In the P_α phase of DOPE, only a ν(ND) band near 2200 cm^{-1} is clearly visible (Figure 2). The sorption of water at the $P_\alpha-H_{II}$ transition is reflected by an enhancement of the $\nu_{13}(D_2O)$ band at about 2500 cm^{-1}. Moreover, the ν(ND) band apparently becomes broader and decreases in intensity. Obviously, a considerable fraction of the direct $N^+D\cdots OP^-$ bonds between phosphate and ammonium groups are broken and replaced by $DOD\cdots OP^-$ and $N^+D\cdots OD_2$ bonds to the water molecules that can be assumed to bridge the polar moieties of DOPE.

The 10% molar fraction of water in the H_2O/D_2O mixture (1:9 mol/mol) leaves some water absorption by isolated O−H stretching vibrations in the spectral range of 3600−3100 cm^{-1}. The position of the ν(OH) band represents a rough measure for the strength of intermolecular interactions of water the more so as isotopic dilution suppresses the inter- and intramolecular vibrational coupling of H−O−H stretches.[30] In the P_α phase, a weak feature protrudes at ∼3480 cm^{-1}. This position is characteristic for weakly H bonded water.[31] At the $P_\alpha-H_{II}$ phase transition a second component at ∼3370 cm^{-1} appears and increases in intensity. It corresponds clearly to water molecules that interact with PE headgroups via H bonds.

H → D exchange also induces a considerable right-hand shift of the ν_{as}(CCN) and ν_s(CCN) bands (Figure 1 and Table 1) because of the bigger mass of ND_3^+ compared to NH_3^+ and because of different degrees of vibrational coupling between ND_3^+ and NH_3^+ deformation modes with CCN stretches (see ref 32 and references therein). The shape of this band apparently

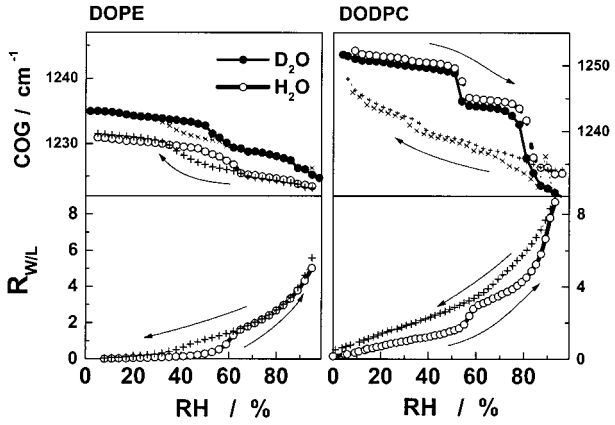

Figure 3. Center of gravity of the antisymmetric PO_2^- stretching vibration of DOPE (left) and DODPC (right) as a function of relative humidity in H_2O and in a D_2O:H_2O (9:1) atmosphere (above) and the corresponding hydration isotherms (below, only H_2O). Hydration and dehydration scans are indicated by circles and crosses, respectively (see also the arrows). $R_{W/L}$ is the number of water molecules sorbed per lipid as determined by gravimetry (see the accompanying paper[20]). Note the correspondence of COG graphs and adsorption isotherms.

transforms from a doublet into a single peak. It should, however, be taken into account that the frequency shift between both subbands ($\Delta\nu \sim 10$ cm^{-1}) is smaller than their full width at half-maximum (>15 cm^{-1}). Hence, band splitting does not necessarily result in two distinct maxima of the subbands. Preliminary band shape analysis of the ν_{as}(CCN) band centered at 969 cm^{-1} reveals a second component in the range 980−975 cm^{-1} (not shown).

The positions of all phosphate bands significantly shift after deuteration. This result shows that the vibrations of the phosphate moieties are affected via $PO\cdots DN^+$ hydrogen bonds. Figure 3 reveals that the effect of H → D exchange on the $\nu_{as}(PO_2)$ band is virtually constant over the whole RH range. Hence, interactions between ammonium and phosphate groups do still exist in the hydrated system. The correlated behavior

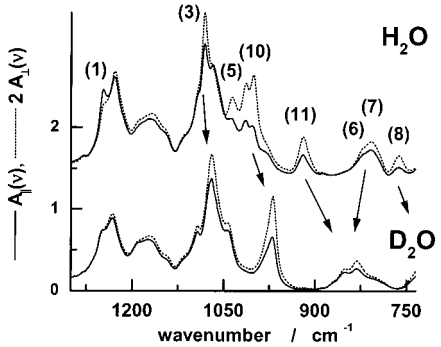

Figure 4. Polarized absorbance spectra, $A_{\parallel}(\nu)$ and $2A_{\perp}(\nu)$, of nearly anhydrous DOPE (RH = 5%, T = 25 °C, P_{α} phase) before and after H → D exchange of the ammonium groups, which was realized in a 9:1 D_2O:H_2O atmosphere. Absorption bands that possess a pronounced dichroism are numbered according to Table 1 (see column "peak number" for assignments). The arrows indicate shifts of band positions after deuteration. Note that the condition $A_{\parallel}(\nu) = 2A_{\perp}(\nu)$ refers to a random orientation of the respective transition moment, for example, because of the absence of macroscopic order of the lipids.

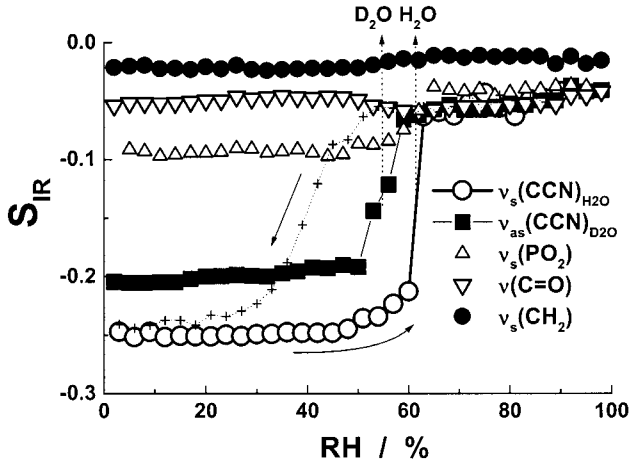

Figure 5. Infrared order parameter of selected absorption bands of the ammonium, phosphate, carbonyl and methylene groups of DOPE as a function of the relative humidity (T = 25 °C, hydration scan, H_2O). The solid symbols refer to the experiment in a D_2O:H_2O (9:1) atmosphere. The respective $P_{\alpha}-H_{II}$ phase transition takes place at a smaller RH value than in the H_2O atmosphere. The center positions of the phase transition are indicated by vertical arrows (RH_{pt} = 55% in D_2O:H_2O and 62% in H_2O). The graph of $S_{IR}(\nu_s(CCN))$ of the dehydration scan is symbolized by crosses.

of the hydration dependence of the spectral parameter $COG(\nu_{as}(PO_2))$ and of the adsorption isotherm (see the accompanying paper for details of the method) indicates that the primary hydration properties of DOPE are dominated by water binding to phosphate groups.

The C═O stretching band, ν(C═O), shifts and broadens only slightly upon "headgroup melting" of DOPE and it remains virtually unaffected after H → D exchange (Figure 1 and Table 1). Carbonyl groups seem to be weakly involved in the H bonding network formed in the polar region of the lipid. Note that the shape and position of the ν(C═O) band vary markedly at the corresponding phase transition of disaturated and diene PE lipids owing to chain melting.[12,27,33]

IR Linear Dichroism of DOPE. The polarized absorption spectra of DOPE reveal a considerable linear dichroism of some of the absorption bands due to headgroups (see Figure 4). This indicates macroscopic ordering of the lipid molecules within aggregates that possess macroscopic orientation at the surface of the ATR crystal. The respective IR order parameters, S_{IR}, are given in Table 1. IR-dichroism measurements of DOPE films on a germanium crystal yield virtually identical S_{IR} data.[23] A specific influence of the chemical nature of different crystal surfaces on the detected structure can be excluded because of the different penetration depth of electromagnetic waves (~0.5 μm for Ge and ~2.5 μm for ZnSe). Finding negative values for the IR order parameter of all the vibrational modes due to the ammonium group is compatible with a predominantly parallel orientation of the respective transition moments with respect to the ATR surface (Table 1). Contrarily, the high-frequency phosphate band due to antisymmetric PO_2^- stretches possesses a positive IR order parameter. The linear dichroism of all these bands remains constant up to the $P_{\alpha}-H_{II}$ phase transition and drops considerably toward zero in the inverse hexagonal phase (Figure 5). The distinct decrease of the absolute values of S_{IR} has been recently used as a characteristic signature to detect lamellar-to-inverse-hexagonal-phase transitions of lipids.[12] In these systems, the dichroism of acyl chains and headgroups changes in a similar fashion, in contrast to DOPE, where the IR order parameters of the methylene and carbonyl groups are close to zero in both H_{II} and P_{α} phases. The absence of significant macroscopic ordering of the acyl chains is confirmed by the polarized spectra in the range of the ν_{as}(COC) mode (1180−1160 cm^{-1}; see Figure 4). This feature gives no indication of a preferential orientation of the ester bonds of the acyl chains. In bilayers, the ν_{as}(COC) band splits typically into two components of positive and negative linear dichroism owing to the different conformation and orientation adopted by the ester bonds of the sn-1 and sn-2 chains.[12,34]

Lyotropic Phase Behavior of DODPC. The lyotropic phase behavior of the diene lipid DODPC was extensively studied by means of IR linear dichroism and X-ray measurements.[11,16,17] In the medium RH range, DODPC transforms between two crystalline subgel phases called SG_I and SG_{II}.[11] The packing of octadecadienoyl chains remains nearly unaffected at the SG_I-SG_{II} transition, whereas direct interactions between the phosphate and trimethylammonium (TMA) groups are broken down because of the hydration of these moieties.[16] Hence, the SG_I-SG_{II} transition represents a sort of headgroup-solvation-induced transition characterized by a considerable increase of the molecular disorder of the trimethylammonium groups. In contrast to DOPE, the headgroup structure changes even in lipid aggregates with crystalline acyl chains (see below).

The relatively narrow IR absorption bands of the ν(OH) and $\nu_{13}(D_2O)$ modes in the SG_I phase (cf. Figure 2) are caused by very few ($R_{W/L}$ = 1−2) highly oriented water molecules that occupy discrete binding sites at the PC headgroups. The headgroup melting is obviously correlated with an increase of the right-hand flank of the ν(OH) and $\nu_{13}(D_2O)$ bands. The one water molecule per lipid that is additionally adsorbed at the solvation-induced transition can be assumed to interact strongly with the lipid via H bonds in correspondence to the respective changes of the water band at the $P_{\alpha}-H_{II}$ transition of DOPE. The experiment in D_2O:H_2O (9:1) reveals that the $\nu_{as}(PO_2)$ frequency of DODPC is less sensitive to the H → D exchange than the $\nu_{as}(PO_2)$ band of DOPE the phosphate group of which to a considerable degree interacts with the amine protons (Figure 3).

Note that DODPC in addition undergoes the lyotropic chain-melting transition at RH > 85% (see next paragraph). This event is then accompanied by a considerable hydration of the lipid (cf. Figure 3).

Hydration of DODPC and DOPE at Different Temperatures: RH−*T* Phase Diagrams. The temperature dependence of the lyotropic headgroup-solvation-induced transition of the

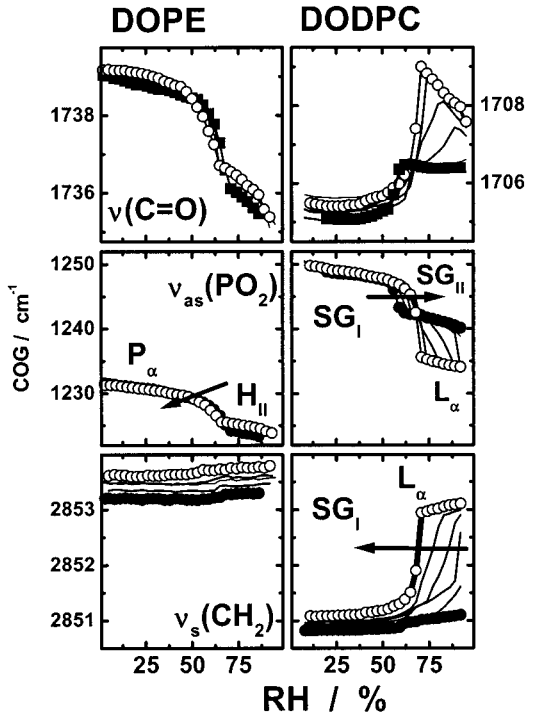

Figure 6. Center of gravity of the ν(C═O), $\nu_{as}(PO_2)$ and $\nu_s(CH_2)$ absorption bands upon hydration of DOPE and DODPC at different temperatures; arrows indicate the shift direction of the $P_\alpha-H_{II}$ (DOPE), the SG_I-SG_{II} and $SG_{II}-L_\alpha$ (DODPC) phase transition with increasing temperature. The minimum (solid symbols) and maximum (open symbols) temperatures are T_{min}/T_{max} = 10 °C/30 °C (DOPE) and 15 °C/40 °C (DODPC). The thin lines correspond to intermediate temperatures that were chosen with an increment of 5 K. Note that $P_\alpha-H_{II}$ and the SG_I-SG_{II} transitions shift in opposite directions upon heating.

lipids was studied by using the frequency shifts of the antisymmetric phosphate stretching vibration, $\nu_{as}(PO_2^-)$, and of the carbonyl stretching band, ν(C═O), at the $P_\alpha-H_{II}$ and SG_I-SG_{II} phase transitions of DOPE and DODPC, respectively (see Figure 6). In the hydration scans, these spectral parameters drop in a fashion characteristic for to PE and PC headgroup melting (see also refs 11 and 14). With increasing temperature the $P_\alpha-H_{II}$ transition of DOPE shifts to smaller RH values and the SG_I-SG_{II} transition of DODPC to larger values of RH (cf. Figure 6, arrows).

Upon an increase in RH, the headgroup-melting transition of DODPC is followed by the chain-melting transition into the liquid-crystalline L_α phase. This event shifts into the opposite direction compared to the SG_I-SG_{II} transition when temperature is varied. Consequently, the RH range occupied by the intermediate SG_{II} phase narrows with increasing temperature. Finally, the SG_I phase converts directly into the L_α state at temperatures of $T > 35$ °C. The conformational change of the polymethylene chains at the solid/liquid-crystalline phase transition gives rise to a considerable increase of the methylene stretching frequency, $\nu_s(CH_2)$, which has been used to determine the RH value of the chain-melting as a function of temperature (Figure 6). However, the $\nu_s(CH_2)$ frequency of both lipids is virtually not affected by the solvation-induced transitions. This provides the clue to study these phase transitions concerning predominantly the lipid headgroups without considerable contributions due to conformational changes of the hydrocarbon chains.

The phase transition data were summarized in Figure 7 in terms of RH−*T* phase diagrams of both lipids.

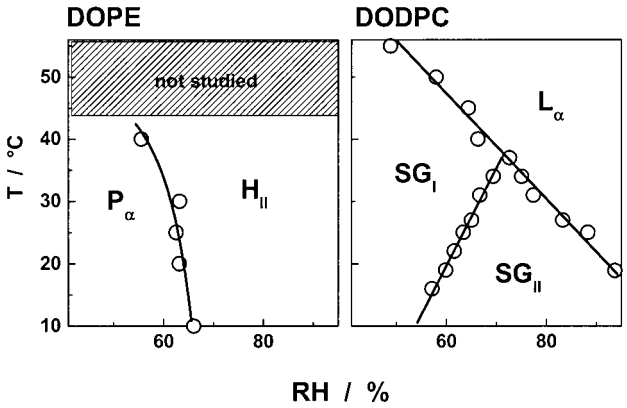

Figure 7. RH−*T* phase diagrams of DOPE and DODPC; the symbols represent experimental data that were obtained by means of infrared spectroscopy (cf. Figure 6).

Discussion

Dimensions of the Lipid Aggregates in the P_α Phase. The IR order parameter gives a measure of the mean orientation of a transition moment with respect to the optical axis. It depends on the ordering and orientation of the molecules within aggregates and on the ordering and orientation of the aggregates on the ATR surface. Under certain conditions both effects can be separated by a set of uniaxial order parameters, such as the order parameter of aggregate morphology, S_d, and the order parameter of local molecular orientation, S_μ (see Appendix). For the inverse hexagonal phase, one obtains for example $S_\mu = S_{IR}/S_d(\text{hex}) \approx 4S_{IR}$. The IR order parameters measured for the vibrations phosphate and carbonyl groups in the H_{II} phase of DOPE ($S_{IR}(\text{hex}) = -0.05 \pm 0.05$, cf. Figure 5), and the respective IR order parameters of fluid lamellar lipid systems ($S_{IR}(\text{lam}) = -0.20 \pm 0.05$[16,36]) yield, in both cases, similar molecular order parameters, $S_\mu = S_{IR}(\text{lam})/S_d(\text{lam}) \approx 1S_{IR} = S_{IR}(\text{hex})/S_d(\text{hex}) \approx -0.2 \pm 0.1$, which indicate a comparably similar degree of molecular order relative to the local director of the different aggregates. A more detailed analysis of the molecular ordering within the H_{II} phase seems, however, not appropriate because of the relatively large uncertainty of the data.

In the P_α phase, the linear dichroism of headgroup modes increases markedly, and thus, a quantitative analysis becomes reasonable. X-ray diffractograms of nearly dry DOPE reveal two first-order Bragg peaks at $1/d_1$ = 1/4.07 nm and $1/d_2$ = 1/4.41 nm,[23] which can be interpreted in terms of a rectangular centered two-dimensional lattice with the spacings a_{lat} = 8.13 nm and b_{lat} = 5.25 nm (see Appendix and Figure 9 for illustration). To analyze linear dichroism, we used the model of rodlike aggregates given in the Appendix. The lattice parameters a_{lat} and b_{lat} yield the rod dimensions a = 4.38 nm and b = 4.90 nm (eq A4 and Figure 9). The axial ratio, r = 1.12, gives the corresponding order parameter of aggregate morphology, S_d = 0.29 (eq A3; see Figure 10). The molecular order within the ribbons can now be evaluated by means of $S_\mu = S_{IR}/S_d \approx 3.5S_{IR}$. This formula yields values of $S_\mu < -0.5$ that are unrealistic for the vibrations of the ammonium group and of the phosphate group, too (Table 1 and Figure 5). From the IR linear dichroism data one can deduce an apparent order parameter of aggregate morphology of $0.5 \le S_d \le 1$ to guarantee realistic values of $S_\mu \ge -0.5$ for all IR modes under investigation. It corresponds to an apparent "spectroscopic" axial ratio of the ribbons of $r > 2$ (cf. Figure 10). Note that the space-

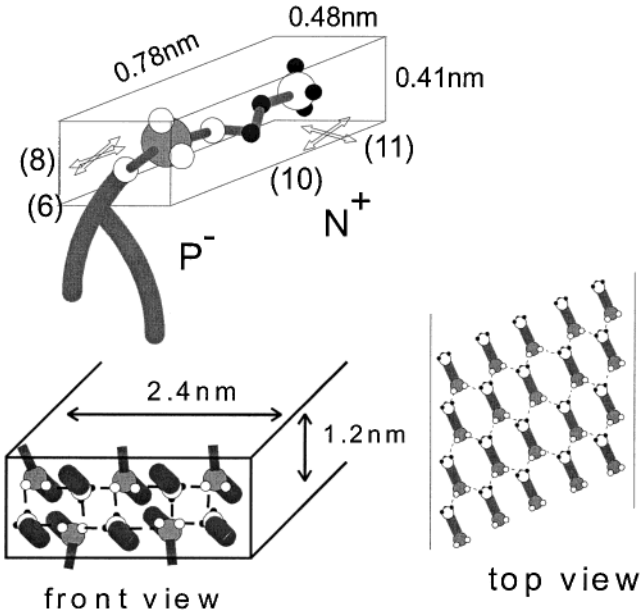

Figure 8. Schematic representations of the dimensions of a PE headgroup in a crystalline lipid system (above) and of the molecular arrangement in a "headgroup" ribbon in the P_α phase of DOPE (below, front and top views). The numbers assign the transition moments of the $\nu_s(CCN)$,[11] $\nu_{as}(CCN)$,[10] $\nu_{as}(P-OC)_2$),[6] and $\nu_s(P-OC)_2$)[8] vibrations that are schematically illustrated by arrows.

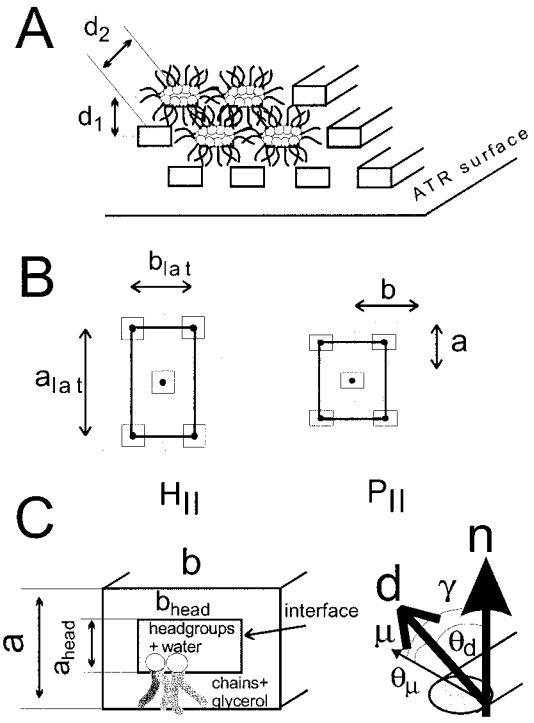

Figure 9. Schematic representation of the geometry of the ribbon phase. The rod-shaped aggregates are oriented with their axes parallel to the surface of an ATR crystal (part A). The dimensions of the rectangular lattice are related to the Bragg spacings, d_1 and d_2, by means of $a_{lat} = 2d_1$ and $b_{lat} = d_2/(1 - (d_1/2d_2)^2)^{0.5}$ (part A and B). The cross section of the headgroup region is indicated by gray rectangles. Part C shows the unit vectors pointing along the ATR normal (**n**), along the normal of the polar/apolar interface (**d**) of a cylindrical aggregate with an ellipsoidal cross section and along the transition dipole (μ). For more details see text.

filling cell model yields $r_{lat} \approx 1.29$ (see Appendix) a value that is also to small to explain the linear dichroism of the headgroup vibrations.

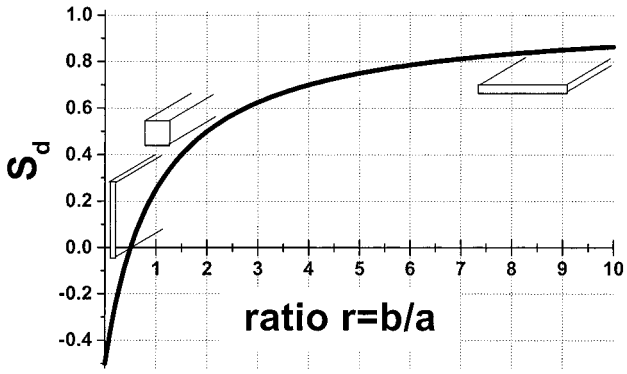

Figure 10. Order parameter of aggregates of rectangular rods, S_d(rect), as a function of the ratio of the lengths of their sides, $r = b/a$ (see Figure 9 and eq A3). Side b aligns parallel with the ATR surface.

The geometrical model obviously underestimates the horizontal dimensions of the ribbons and/or orientations of the local director parallel with respect to the optical axis. We conclude that (i) the molecules do not evenly distribute over the surface of the polar rods and/or (ii) the cross section of the polar rods is flattened in vertical direction when compared with the rod dimensions derived from the lattice geometry.

Molecular Packing within the Ribbons. One DOPE molecule binds, on the average, less than 0.5 water molecules in the ribbon phase (see Figure 3). Hence, PE headgroups form a virtually anhydrous, rigid structure that is stabilized by a network of direct H bonds between the ammonium and phosphate groups as has been shown by the IR spectra obtained before and after $H \rightarrow D$ exchange (vide supra). X-ray single-crystal analyses of 3-palmitoyl-glycero-1-phosphoethanoloamine (PPE) and of 2,3-dilauroyl-glycero-phosphoethanolamine acetic acid (DLPE) reveal a parallel and antiparallel staggered pattern of the headgroup dipoles in a lamellar arrangement, respectively, in which two of the hydrogens of each ammonium group interact laterally with neighboring phosphate groups.[36-38] Each PE group orients parallel to the surface of a layer and occupies an area of $A_{PE} = 0.78\ nm \times 0.48\ nm = 0.35-0.39\ nm^2$ (see Figure 8 for illustration). It appears reasonable to assume a similar headgroup structure in the P_α phase of DOPE because of the quasi-crystalline character of the phosphate and ammonium vibrations. Making use of the specific volume of a PE headgroup of ~0.67 cm^3/g (see ref 18 and references therein), one obtains a rough measure of their mean volume, $v_{head} \approx 0.156\ nm^3$, and of their mean vertical dimension of 0.41 nm.

Equation A5 yields the tentative dimensions of the headgroup ribbons, $a_{head} \approx 1.6$ nm and $b_{head} \approx 1.8$ nm, assuming a specific and a molecular volume of DOPE of 1 cm^3/g and of $v_L \approx 1.2\ nm^3$, respectively. The roughly rectangular profile of the PE group suggests that optimal packing should be with the long dimensions more parallel and with their short dimensions more perpendicular to the ribbons. Consideration of both dipole-dipole interactions and lateral hydrogen bonding and comparison of lateral dimensions of the headgroup ribbons with those of the PE headgroups has led us to assume that the PE groups fit into the ribbons in a sandwich-like structure. That means, about 3-4 PE groups would stack side by side on each of the two opposite broad sides of ribbons. The vertical rod dimension of $a_{head} \approx 1.6$ nm however clearly exceeds the vertical extension of two parallel headgroup layers (~0.8 nm).

From the linear dichroism of the headgroup modes we deduced an axial ratio of $r \geq 2$ (vide supra). It corresponds to a deformation of the polar ribbons in vertical direction. If one assumes constant volume (and cross section) of the polar ribbons

($A = a_{head}b_{head} = \text{const}$) a simple estimation yields $a_{head} \leq 1.2$ nm and $b_{head} \geq 2.4$ nm. These data are compatible with 8−12 DOPE molecules that pack around the cross section of the ribbons. Scherer estimated a maximum of 10 PE lipids arranging around the perimeter of the hydrophilic tube of the H_{II} phase of PE lipids at zero hydration.[39] This number is within the error limits of our estimation. Recently, we found that the inverse hexagonal phase of DTDPE, a PE lipid with tetradecadienoyl chains, also transforms into the P_α phase at nearly dry conditions ($T = 45$ °C, $R_{W/L} < 1$[40]). From the respective Bragg spacings ($d_1 = 3.22$ nm, $d_2 = 3.38$ nm[40]) and a molecular volume of $v_L = 1.05$ nm^3, we derived dimensions of headgroup ribbons ($a_{head} \leq 1.0$ nm and $b_{head} \geq 2.0$ nm) resembling that of DOPE (vide supra). These results give rise to two conclusions. First, the packing and the intermolecular interactions between PE headgroups mainly determine the structure of the aggregates. Second, the headgroups locally arrange in a nearly lamellar fashion.

Valuable information about the headgroup orientation in lipid systems can be deduced by assuming the existence of isolated group vibrations.[16,25,35] In the frame of this model, the transition moments of the symmetric and antisymmetric stretching modes in a triatomic fragment, $\mu(\nu_s)$ and $\mu(\nu_{as})$, are oriented within the plane formed by the atoms with $\mu(\nu_s)$ and $\mu(\nu_{as})$ pointing more parallel and more perpendicular in relation to the bisectrice of the binding angle, respectively. Consequently, the negative, similar IR order parameters of the symmetric and antisymmetric C−C−N stretches (cf. Table 1) indicate that the C−C−N plane aligns predominantly parallel with the polar interface of the aggregates.

The S_{IR} values of the symmetric vibrations of the phosphate group are significantly smaller (more negative) than the respective antisymmetric modes, i.e., $S_{IR}(\nu_s(P{-}OC)_2) < S_{IR}(\nu_{as}(P{-}OC)_2)$ and $S_{IR}(\nu_s(PO_2) < S_{IR}(\nu_{as}(PO_2))$. This result can be interpreted in terms of an oblique orientation of the (CO)−P−(OC) plane accompanied by an asymmetric position of the two nonesterified oxygens with respect to the interface. The left-hand sharp component of the $\nu_{as}(PO_2)$ band has been tentatively assigned to phosphates that are not or only weakly involved in H bonding to the ammonium groups (vide supra). Its positive IR order parameter, $S_{IR}(\nu_{as}(PO_2)_{1245}) > 0.1$, may indicate a different orientation of the respective phosphate groups. Alternatively, the two-component nature of the $\nu_{as}(PO_2)$ band could be explained in terms of H bonding asymmetric with respect to the two oxygens. In an OPO···H structure, the left O−P bond bears the characteristics more close to a P═O double bond. Its frequency is expected to increase and its transition moment would shift toward a position more parallel to the P═O bond, and, thus, become more perpendicular relative to the interface. In qualitative agreement with our interpretation of the IR-dichroism data of DOPE, the crystal structures of DLPE and PPE reveal networks of H bonds that are asymmetric with respect to obliquely oriented phosphate groups.[36] Fringeli argued in favor of protonated phosphate groups in dry dipalmitoyl DPPE films, i.e., a uncharged O═P−OH···NH_2 structure.[41] The corresponding spectra show a ||-polarized subband at 1256 cm^{-1}. Note that, by contrast, the IR linear dichroism of PC headgroups is compatible with a symmetric mean orientation of the phosphate group.[16,35]

The IR order parameters of all vibrations of the acyl chains adopt values near zero also in the P_α phase. The chains obviously possess a highly disordered structure that includes the carbonyl-ester groups as well. The absence of macroscopic molecular order of the CO−O fragments can be explained by different conformations of this moiety in DOPE molecules that are located either in the center or at the edges of ribbons. Although the PE headgroups arrange into a locally lamellar structure, the disordered chains prevent the formation of a lamellar phase because of the mismatch between the small area requirement of the headgroups and the distinctly larger area spanned by the projection of the fluid chains into the interfacial plane. On the other hand, the relatively strong interactions between the PE headgroups prevent the formation of the inverse hexagonal phase with hydrophilic rods of a circular cross section.

Structure of the Polar Region of DODPC Membranes. At room temperature the diene lipid DODPC forms exclusively lamellar phases the molecular structure of which was extensively studied by means of IR linear dichroism and X-ray diffraction.[11,16,17] It was found that the rigid, platelike diene groups tend to stack parallel to each other. At low hydration, this property causes a cooperative transformation of the dienoyl chains into a dense, crystalline packing motif with tilted acyl-chain axes owing to conformational restrictions near the diene groups. These packing requirements of octadecadienoyl chains force the area of the polar/apolar interface to increase in a fashion atypical for usual PC lipids. The large surface area facilitates the trimethylammonium (TMA) groups to reside closer to the hydrocarbon boundary. The resulting in-plane orientation of the headgroups enables a closer approach between the phosphate and TMA groups of neighboring molecules. Thus, terminal TMA groups immobilize, and the whole PC group dehydrates because the attractive Coulombic forces between the oppositely charged moieties become very effective and, moreover because of contacts between the phosphate oxygens and the methyl hydrogens arise.[42]

Hence, the headgroups of both investigated lipids, DOPE and DODPC, tend to orient preferentially parallel with respect to the polar interface at low hydration. The IR order parameters of selected absorption bands of the phosphate and trimethylammonium groups of DODPC and of DOPE are compared in Table 1. The in-plane orientation of the headgroup of DODPC in the SG_I phase is somewhat unusual because PC headgroups typically incline with respect to the membrane surface giving rise to a clearly positive IR order parameter of the $\nu_{as}(P{-}(OC)_2)$ vibration in both liquid-crystalline and gel phases.[16,35]

Solvation-Induced Transitions of PE and PC Headgroups. At the $P_\alpha{-}H_{II}$ phase transition, each DOPE molecule additionally binds about one water molecule (cf., Figure 3 and ref 20). The broadening and the shift of the ammonium and phosphate bands accompanying this process indicate that the interactions between these moieties drastically change due to a partial solvation of PE headgroups. The formation of a nearly anhydrous network of headgroups is characteristic of disaturated PE lipids at low water activities.[27,37,38,43] In DOPE, headgroups form a rigid structure even in the presence of fluid hydrocarbon chains. Consequently, the $P_\alpha{-}H_{II}$ phase transition should be attributed to an intrinsic property of the PE headgroups that is not superimposed by chain melting. In other words, this event represents a sort of lyotropic "headgroup melting" transition.

Each DODPC molecule also imbibes one water molecule at the $SG_I{-}SG_{II}$ phase transition. Headgroup solvation was evidenced from distinct changes of both width and linear dichroism of the IR absorption bands of trimethylammonium groups.[11,16] In contrast to DOPE, the formation of a rigid PC headgroup structure is, however, induced by the freezing of acyl chains into a more dense, paraffin-like packing mode. However, the solvation-induced transition of DODPC affects the solid structure of the hydrophobic core of the membranes only slightly.[11]

Hence, the SG_I-SG_{II} transition of DODPC proceeds between two closely related lamellar phases whereas the $P_\alpha-H_{II}$ transition of DOPE is accompanied by a considerable deformation of the aggregates, i.e., a dramatic change of their morphology. It was shown that D_2O slightly increases the gel-to-liquid-crystalline-phase transition temperature of PC and PE lipids at full hydration probably because of stronger hydrogen bonds that stabilize the gel state.[44−47] Contrarily, the transition temperature from the lamellar to the inverted hexagonal phase of lipids is significantly depressed up to about 5 K when H_2O was exchanged by D_2O.[47] In this case, stronger hydrogen bonds between the PE headgroups can be assumed to increase the inverse curvature strain within the lipid monolayers. Thus, H → D exchange may promote the bending of lamellae into inversely curved aggregates. We observed a similar effect of D_2O on the lyotropic $P_\alpha-H_{II}$ transition of DOPE. The RH value of the phase transition decreases significantly by 4−6% in a D_2O atmosphere (Figure 5). Hence, the $P_\alpha-H_{II}$ phase transition possesses the characteristics of a lamellar-to-inverse-hexagonal transition at least with respect to this property. This result can be judged as an additional argument in favor of a pseudo-layered arrangement of PE headgroups in the P_α phase.

Note that D_2O has no significant effect on the lyotropic phase transitions of DODPC. The interactions between water (H_2O or D_2O) and the polar moieties of this lipid are obviously less important than the direct interactions between PE headgroups.

Summary and Conclusions

We have characterized the structure and interactions of phosphatidylethanolamine and phosphatidylcholine headgroups in aggregates of selected unsaturated lipids. Both different types of moieties undergo a lyotropic solvation-induced transition in the intermediate range of relative humidity. Interestingly, both lipids maintain the order states of their acyl chains independently of the hydration state and/or the phase adopted: accordingly, the phases appear to be consistently solid for DODPC and fluid for DOPE. Consequently, the hydration of the headgroups could be studied without significant interference of chain-melting. From a structural point of view a highly ordered, quasi-crystalline arrangement of nearly anhydrous lipid headgroups transforms into a more disordered arrangement of hydrated headgroups in both cases. Direct interactions between the polar groups of the lipids break at least in part and become substituted by and/or mediated via water molecules.

At low water activities, the headgroups of both investigated lipids tend to orient preferentially parallel with respect to the polar interface as revealed by infrared linear-dichroism data. Furthermore, the latter results are compatible with assuming the formation of a rectangular centered phase for water-depleted DOPE. The cross-section layers of the inverted ribbons involve 8−12 DOPE molecules according to model considerations. The PE groups are stabilized mainly by particularly strong, "locked" hydrogen bonds whereas the PC moieties preferentially interact via "salt bridges", i.e., electrostatic attraction.

In the following second part of this publication, the thermodynamic aspects of this difference will be reported.[20]

Acknowledgment. This work was supported by the Deutsche Forschungsgemeinschaft within SFB 294 (TP C7) and SFB 197 (TP A10 and B10).

Appendix

IR Linear Dichroism of Nonlamellar Phases and Aggregate Dimensions. Let us introduce the unit vectors **n**, **d** and $\boldsymbol{\mu}$ pointing along the normal of the ATR surface, along the local director and along the IR-active transition moment, respectively. The local director is defined as the normal of the interface that divides the polar and apolar parts of the lipid aggregates. The IR order parameter can be expressed as the product of nested, uniaxial distributions if macroscopic ordering possesses cylindrical symmetry with respect to **n** and if the relative orientations of **n**, **d** and $\boldsymbol{\mu}$ are independent of each other:

$$S_{IR} = S_d S_\mu \tag{A1}$$

The IR order parameter (S_{IR}), the order parameter of aggregate morphology (S_d), and the order parameter of molecular orientation (S_μ) are defined as the second-order Legendre polynomial, $P_2(x) \equiv 0.5(3\cos^2 x - 1)$, of the angles enclosed between $\boldsymbol{\mu}$ and **n** ($S_{IR} \equiv \langle P_2(\gamma)\rangle$), **d** and **n** ($S_d \equiv \langle P_2(\theta_d)\rangle$) and $\boldsymbol{\mu}$ and **d** ($S_\mu \equiv \langle P_2(\theta_\mu)\rangle$) (see Figure 9 for illustration). The angular brackets denote ensemble averaging over all relative orientations existing in the sample. The distribution function of relative orientations, $f(x)$, gives the probability that the orientation with the angle x exists. For example, the order parameter S_d is defined as

$$S_d \equiv \int_0^{\pi/2} P_2(\theta_d)\, f(\theta_d)\, d\theta_d \tag{A2}$$

The function $f(\theta_d)$ can be deduced from the morphology of lipid aggregates. In the present context, we make use of the mean shape of the polar/apolar interface and assume that the lipid molecules are evenly distributed over the interface (see Figure 9). For spherical, lamellar and cylindrical aggregates one obtains $S_d(\text{sph}) = 0$ ($f(\theta_d) = \sin\theta_d$), $S_d(\text{lam}) = 1$ ($f(\theta_d) = \delta(0)$, $\delta(x)$ is the delta function) and $S_d(\text{cyl}) = 0.25$ ($f(\theta_d) = 2/\pi$), respectively. In the latter two cases it was assumed that the lamellae and the long axes of the cylinders align parallel with respect to the ATR surface. For rods possessing a quadratic ($S_d(\text{qua}) = 0.5(P_2(0) + P_2(\pi/2)) = 0.25$) and a hexagonal ($S_d(\text{hex}) = {}^1/_3(P_2(0) + 2P_2(\pi/3) = 0.25$) cross section perpendicular to their long axes one obtains identical values of $S_d = 0.25$.

For rods with a rectangular cross section of side ratio $r = b/a$, the order parameter becomes

$$S_d(\text{rect}) = \frac{a}{a+b}\left(\frac{b}{a}P_2(0) - 0.5P_2\left(\frac{\pi}{2}\right)\right) = \frac{1}{r+1}(r - 0.5) \tag{A3}$$

if side b orients parallel to the surface of the ATR crystal. Figure 10 shows S_d as a function of the axial ratio.

Our treatment neglects disordering effects such as imperfect alignment of lipid aggregates with the ATR surface and/or undulations of the polar/apolar interface. These effects can be taken into account by additional multiplicative order parameters in eq A1.

In the inverse hexagonal phase, the axes of cylindrical aggregates form a two-dimensional rectangular lattice of dimensions a_{lat} and $b_{lat} = a_{lat}/\sqrt{3}$ (cf. Figure 9b). The assumption of a circular, hexagonal or quadratic cross section of the cylinders is equivalent with respect to the order parameter of aggregate morphology (vide supra). For the sake of simplicity let us consider quadratic rods with a cross-sectional area ($A = a^2$) equal to the area of cylindrical aggregates in a corresponding space filling cell model ($A = a_{lat}b_{lat}/2 = a_{lat}^2/(2\sqrt{3})$, see, e.g., ref 48). The side length of the quadratic rods are $a = b = \sqrt{A} = a_{lat}/(2\sqrt{3})^{0.5}$. The quadratic rods transform into rectangular ones with

$$a = a_{lat}/(2\sqrt{3})^{0.5} \quad \text{and} \quad b = b_{lat}(\sqrt{3}/2)^{0.5} \tag{A4}$$

if the hexagonal lattice deformes in vertical directions. The newly formed lattice pertaining the ribbon phase is of centered rectangular symmetry.[49] The ratio of vertical and horizontal dimensions of the "spectroscopic" ribbons, $r = \sqrt{3}b_{lat}/a_{lat}$, differs from the ratio of dimensions of the respective space-filling cell model, $r_{lat} = 2b_{lat}/a_{lat}$, by the geometric factor $\sqrt{3}/2$.

The ribbonlike aggregates with rectangular cross section can be divided into regions that enclose the lipid headgroups and the adsorbed water on one hand, and the acyl chains and the glycerol moiety of the lipid on the other hand. In a simple model we consider "headgroup" rods the dimensions of which are proportional to the volume fraction of the headgroup (+water), $f_{head} = (\upsilon_{head} + R_{W/L}\upsilon_W)/(\upsilon_L + R_{W/L}\upsilon_W)$ (see Figure 9, V_L and υ_W denote the molecular volume of the lipid and of water, respectively; υ_{head} is the respective volume of the headgroup), i.e.

$$a_{head} = a\sqrt{f_{head}} \qquad \text{and} \qquad b_{head} = b\sqrt{f_{head}} \qquad \text{(A5)}$$

References and Notes

(1) Langner, M.; Kubica, K. *Chem. Phys. Lipids* **1999**, *101*, 3.
(2) Cevc, G. J. *Chem. Soc., Faraday Trans.* **1991**, *97*, 2733.
(3) Rand, P. *Annu. Rev. Biophys. Bioeng.* **1981**, *10*, 277.
(4) Arnold, K. Cation-induced vesicle fusion modulated by polymers and protein. In *Handbook of Biological Physics*; Lipowski, R., Sackmann, E., Eds.; Elsevier Science B. V.: Amsterdam, 1995; p 903.
(5) Yeagle, P. L. Membrane fusion intermediates. In *Current Topics in Membranes*; Epand, R. M., Ed.; Academic Press: San Diego, 1998; Vol. 44, p 375.
(6) White, S. H.; Wimley, W. C. *Biochim. Biophys. Acta* **1998**, *1376*, 339.
(7) Israelachvili, J. N.; Wennerström, H. *J. Phys. Chem.* **1992**, *96*, 520.
(8) Pasenkiewicz-Gierula, M.; Takaoka, Y.; Miyagawa, H.; Kitamura, K.; Kusumi, A. *Biophys. J.* **1999**, *76*, 1228.
(9) Fitter, J.; Lechner, R. E.; Dencher, N. A. *J. Phys. Chem. B* **1999**, *103*, 8036.
(10) Selle, C.; Pohle, W.; Fritzsche, H. *J. Mol. Struct.* **1999**, *480−485*, 401.
(11) Binder, H.; Anikin, A.; Kohlstrunk, B.; Klose, G. *J. Phys. Chem. B* **1997**, *101*, 6618.
(12) Binder, H.; Anikin, A.; Lantzsch, G.; Klose, G. *J. Phys. Chem. B* **1999**, *103*, 461.
(13) Pohle, W.; Selle, C.; Fritzsche, H.; Binder, H. *Biospectroscopy* **1998**, *4*, 267.
(14) Pohle, W.; Selle, C. *Chem. Phys. Lipids* **1996**, *82*, 191.
(15) Binder, H.; Kohlstrunk, B.; Heerklotz, H. H. *J. Colloid Interface Sci.* **1999**, *220*, 235.
(16) Binder, H.; Gutberlet, T.; Anikin, A.; Klose, G. *Biophys. J.* **1998**, *74*, 1908.
(17) Binder, H.; Kohlstrunk, B. *Vibr. Spectrosc.* **1999**, *21*, 75.
(18) Rand, R. P.; Parsegian, V. A. *Biochim. Biophys. Acta* **1989**, *988*, 351.
(19) Shalaev, E. Y.; Steponkus, P. L. *Biochim. Biophys. Acta* **1999**, *1419*, 229.
(20) Binder, H.; Kohlstrunk, B.; Pohle, W. *J. Phys. Chem. B* **2000**, *104*, 12049.
(21) Binder, H.; Schmiedel, H. *Vibr. Spectrosc.* **1999**, *21*, 51.
(22) Gawrisch, K.; Parsegian, V. A.; Hajduk, D. A.; Tate, M. W.; Gruner, S. M.; Fuller, N. L.; Rand, R. P. *Biochemistry* **1992**, *31*, 2856.
(23) Selle, C. Untersuchung zur Hydratisierung von Phospholipidfilmen mittels der FTIR−Spektroskopie und anderer physikochemischer Methoden. Promotion, FSU, 1999.
(24) Casal, H. L.; Mantsch, H. H. *Biochim. Biophys. Acta* **1984**, *779*, 381.
(25) Fringeli, U. P.; Günthard, H. H. *Mol. Biol. Biochem. Biophys.* **1981**, *31*, 270.
(26) Mantsch, H. H.; Hsi, S. C.; Butler, K. W.; Cameron, D. G. *Biochim. Biophys. Acta* **1983**, *728*, 325.
(27) Lewis, R. N. A. H.; McElhaney, R. N. *Biophys. J.* **1993**, *64*, 1081.
(28) Leberle, K.; Kempf, I.; Zundel, G. *Biophys. J.* **1989**, *55*, 637.
(29) Stewart, J. E. *J. Chem. Phys.* **1959**, *30*, 1258.
(30) Zundel, G. *Hydration and Intermolecular Interactions*; Academic Press: New York, 1969.
(31) Boicelli, C. A.; Giomini, M.; Giuliani, A. M. *Appl. Spectrosc.* **1984**, *4*, 537.
(32) Fringeli, U. P.; Müldner, H. G.; Günthard, H. H.; Gasche, W.; Leuzinger, W. *Z. Naturforsch.* **1972**, *27b*, 780.
(33) Mantsch, H. H.; Martin, A.; Cameron, D. G. *Biochemistry* **1981**, *20*, 3138.
(34) Binder, H. *Vibr. Spectrosc.* **1999**, *21*, 151.
(35) Binder, H.; Arnold, K.; Ulrich, A. S.; Zschörnig, O. *Biophys. Chem.*, submitted for publication.
(36) Pascher, I.; Lundmark, M.; Nyholm, P.-G.; Sundell, S. *Biochim. Biophys. Acta* **1992**, *1113*, 339.
(37) Hauser, H.; Pascher, I.; Pearson, R. H.; Sundell, S. *Biochim. Biophys. Acta* **1981**, *650*, 21.
(38) Hitchcock, P. B.; Mason, R.; Thomas, K. M.; Shipley, G. G. *Proc. Natl. Acad. Sci. U.S.A.* **1974**, *71*, 3036.
(39) Scherer, J. R. *Biophys. J.* **1989**, *55*, 965.
(40) Binder, H.; Dietrich, U.; Schalke, M.; Pfeiffer, H. *Langmuir* **1999**, *15*, 4857.
(41) Fringeli, U. P. *Z. Naturforsch.* **1977**, *32c*, 20.
(42) Grdadolnik, J.; Kidric, J.; Hadzi, D. *Chem. Phys. Lipids* **1991**, *59*, 57.
(43) Pohle, W.; C.; S.; Fritzsche, H.; Bohl, M. *J. Mol. Struct.* **1997**, *408/409*, 273.
(44) Chen, C. H. *J. Phys. Chem.* **1982**, *86*, 3559.
(45) Lipka, G.; Chowdry, B. Z.; Sturtevant, J. M. *J. Phys. Chem.* **1984**, *88*, 5401.
(46) Ma, L. D.; Magin, R. L.; Bacic, G.; Dunn, F. *Biochim. Biophys. Acta* **1989**, *978*, 283.
(47) Epand, R. M. *Chem. Phys. Lipids* **1990**, *52*, 227.
(48) Hagslätt, H.; Söderman, O.; Jönsson, B. *Liq. Cryst.* **1992**, *12*, 667.
(49) Seddon, J. M. *Biochim. Biophys. Acta* **1990**, *1031*, 1.